Enhanced Switching Stability in Ta_2O_5 Resistive RAM by Fluorine Doping

N. Sedghi[1], H. Li[3], I. F. Brunell[2], K. Dawson[2], Y. Guo[3, 4], R. J. Potter[2], J. T. Gibbon[5], V. R. Dhanak[5], W. D. Zhang[6], J. F. Zhang[6], S. Hall[1], J. Robertson[3], and P. R. Chalker[2 a)]

[1]*Department of Electrical Engineering and Electronics, University of Liverpool, Liverpool, L69 3GJ, United Kingdom.*

[2]*School of Engineering, University of Liverpool, Liverpool, L69 3GH, United Kingdom.*

[3]*Department of Engineering, University of Cambridge, Cambridge, CB2 1TN, United Kingdom*

[4]*College of Engineering, Swansea University, Swansea, SA1 8EN, United Kingdom*

[5]*Department of Physics, University of Liverpool, Liverpool, L69 7ZE, United Kingdom*

[6]*Department of Electronics and Electrical Engineering, Liverpool John Moores University, Liverpool, L3 3AF, United Kingdom*

The effect of fluorine doping on the switching stability of Ta_2O_5 resistive random access memory devices is investigated. It shows that the dopant serves to increase the memory window and improves stability of the resistive states due to the neutralization of oxygen vacancies. The ability to alter the current in the low resistance state with set current compliance coupled with large memory window makes multilevel cell switching more favorable. The devices have set and reset voltages of < 1 V with improved stability due to the fluorine doping. Density functional modeling shows that the incorporation of fluorine dopant atoms at the two-fold O vacancy site in the oxide network removes the defect state in mid band gap, lowering the overall density of defects capable of forming conductive filaments. This reduces the probability of forming alternative conducting paths, and hence improves the current stability in the low resistance states. The doped devices exhibit more stable resistive states in both dc and pulsed set and reset cycles. The retention failure time is estimated to be a minimum of 2 years for F-doped devices measured by temperature accelerated and stress voltage accelerated retention failure methods.

There is increasing interest in resistive random access memory (RRAM) as a potential substitute for existing non-volatile memory (NVM). In RRAM devices incorporating metal oxides, switching between different resistive states takes place by field-assisted diffusion of defect sites, usually oxygen vacancies (O_{vac}), producing a conductive filament (CF), which is formed, ruptured, and restored by applying the appropriate voltages[1, 2]. Control of the O_{vac} profile in the oxide film, therefore, is crucial to improve the device performance. The key requirements

a) Author to whom correspondence should be addressed. Electronic mail: pchalker@liverpool.ac.uk

are a large switching memory window for noise immunity and stability of resistive states. Atomic doping with different elements such as N, Ti, Au, Cu, Gd, Si has been reported as an efficient method to modify the oxygen vacancy profile and their movement in forming the conductive paths.[3-11] Recently the doping of dielectrics with fluorine has attracted attention because its electronegativity can significantly influence the energy of mid bandgap states which affects charge trapping and mobility.[12-16] In this work we have used atomic layer deposition (ALD) to fabricate fluorine doped Ta_2O_5 films, which shows a widening of the switching memory window by up to four orders of magnitude together with improved resistive states stability, endurance, and retention time. This improvement is realized by reducing the high resistance state (HRS) current, due to the elimination of excess conduction paths by passivating oxygen vacancies with fluorine dopant atoms.

The amorphous tantalum oxide based metal-insulator-metal (MIM) structures were fabricated on Corning glass or silicon wafer substrates. The devices comprise of a bottom electrode of 50 nm Pt, with a 10 nm Cr adhesion layer, deposited by dc magnetron sputtering, the oxide layer, 15 nm thick Ta_2O_5 or F-doped Ta_2O_5 deposited by conventional ALD, using the precursor $Ta(OC_2H_5)_5$ and H_2O as an oxidant, and the top electrode of 30 nm Ti, with a 60 nm Pt capping layer, deposited by rf sputtering. In-situ F doping was achieved using an aqueous NH_4F solution as a co-reagent and as a substitute for pure water in the ALD deposition process. Substituting 100% of the co-reagent cycles with the NH_4F solution results in an upper F atomic concentration of 1 %, as estimated from X-ray photoelectron spectroscopy (XPS). Conventional photolithography and metal lift-off were used to define the top and bottom contacts and device active area of 512 overlapping and 512 cross-line square devices on each sample, with dimensions of 2 to 150 μm. The plan view optical microscope image of a group of 4 devices and a transmission electron microscopy (TEM) cross section image of a device are shown in Fig. 1. The dc set-reset cycles were performed by return sweeps of a dc voltage from 0 V to a positive value, applied to the Ti contact, for set and to a negative value for reset, using either HP 4155A or Agilent B1500A Semiconductor Parameter Analyzers. The LRS resistance was programmed by setting the current compliance during the set cycle. The resistance at each resistive state was calculated at a 'read' voltage of – 0.1 V. The temperature accelerated retention failure measurements were performed at elevated temperatures up to 250 °C on a heated stage using a Signatone S-1060 temperature controller. The variation of state resistance with time, up to 10^5 s at logarithmically spaced intervals, was calculated from the measured current in sampling mode at a read voltage of – 0.1 V. The applied voltage was kept at 0 V between the sampling intervals to minimize the disturbance of the state current with voltage. For constant voltage stress (CVS)

accelerated failure measurement, the appropriate hold voltage was applied between sampling intervals. The pulsed set and reset endurance measurements, up to 1 million cycles, were performed using an Agilent 33522A function generator, Agilent DSO7012B oscilloscope, and a multi-gain transresistance amplifier with current limit circuit, designed in-house. The statistical variability of each programmed state was analyzed after performing 30 alternate set and reset cycles, for dc sweeps, and up to 1 million cycles, for pulsed sweeps, and calculating the cumulative distribution function (CDF) of resistance at each state.

Typical dc sweep set-reset cycles of the devices made of undoped and F-doped Ta_2O_5 with various proportions of doping cycles are shown in Fig. 2 (a). A significant increase in memory window is caused by fluorine doping due to a reduction in the high resistance state (HRS) current and increase in low resistance state (LRS) current, as shown in Fig. 2 (a, b).

We have previously reported the properties of O_{vac} in the λ phase of Ta_2O_5 crystal and in the amorphous Ta_2O_5 network.[17-19] It has been shown that 2-fold O_{vac} requires the lowest formation energy and smallest energy barrier during diffusion. Therefore, the 2-fold O_{vac} is believed to be responsible for the resistive switching behaviour in the Ta_2O_5 RRAM. In this paper, screened exchange (sX) density functional simulations are used to investigate the incorporation of F dopant atoms in the oxide network, while retaining the correct band gap. The simulation settings are the same as in our previous work.[18] The atomic model and the density of states (DOS) of the 2-fold O_{vac} in amorphous Ta_2O_5 are shown in Fig. 3 (a, b). The removal of the O in the Ta_2O_5 network leaves dangling bonds on the two nearby Ta atoms, which gives a defect state in the mid-gap region. The sX simulation shows that the defect orbital is localized on only one Ta atom. When the F atom is introduced into the network, it takes the place of this O_{vac}, and forms a bond with a Ta atom. The DOS calculation shows such a doping process removes the original O_{vac} defect state in the mid-gap region, thus passivating the O_{vac} defect.[20] The passivation occurs because the doped F atom accepts one electron originally localized at O_{vac} site, while the remaining electron stays at Ta region with the state just below the conduction band minimum. The remaining electron can easily be transferred away due to its high energy state and leave a positively charged F doped center. The reduction of O vacancy densities through passivation serve to reduce the number of excess conduction paths[20] and reduces variability in the LRS current by preventing the setting of the device through a different conduction path in successive set-reset cycles. It also makes the filament denser which increases the LRS current due to a larger conductance and decreases the HRS current due

to a larger gap in the ruptured filament in the critical filament region.[21] When the proportion of doping cycles exceeds 50% the change in HRS or LRS current or resistance is less emphatic, as shown in Fig. 2 (a, b).

The variation of dc sweep set-reset cycles of an F-doped device with set current compliance follows a linear relationship between LRS resistance and set current, as shown in Fig. 4 (a). Figure 4 (b) shows the cumulative distribution function of LRS and HRS resistance at different values of set current compliance. They show a relatively small variation in LRS resistance, but a larger one in the HRS resistance. The latter is a characteristic of filament type RRAM devices due to variability in length of a ruptured filament. By increasing the set current compliance the HRS distribution shifts to a smaller resistance and shows larger variation because the gap in the critical filament region after reset is shorter at larger set currents, resulting in a larger HRS current. The LRS distribution at different set currents exhibits reasonable separation with each other and from the HRS distributions, which indicates the device could be used for multilevel cell (MLC) switching applications. The cumulative distribution functions (CDF) of set and reset voltages are shown in Fig. 4 (c). They show low voltage (< 1 V) set and reset with improved variability compared to undoped devices (not shown).

The LRS and HRS resistances of an F-doped device at three different current compliance values, for 2000 pulsed set and reset cycles read at - 0.1 V, are shown in Fig. 5 (a). The input and output pulse waveforms are shown as inset. The corresponding probability distribution plots in Fig. 5 (b) (symbols) show enhanced stability of resistive state compared to the undoped device (lines). The F-doped device has a pulse set and reset endurance of more than one million cycles as shown by the symbols in the CDF plots of Fig. 5 (c). The measured devices do not fail to set or reset in one million cycles, despite slight variation in states, which reduces the memory window in some regions. By contrast, the endurance of the undoped device is less than 100,000 cycles and it completely fails to set after 500,000 cycles and stays in high resistance state. It was noted, however, that some devices resumed switching after a few more hundred thousand cycles. The corresponding probability plots for a typical undoped device are shown in Fig. 5 (c) (lines) for comparison. It not only has around 30% failure to switch, but also the LRS and HRS resistances have around 75% overlap compared to 2% for F-doped devices.

The metal oxide based RRAM devices have a very long retention time in the range of years which cannot be measured conveniently, so the temperature accelerated failure and constant voltage stress (CVS) accelerated

failure methods were used to reduce the retention failure time. The HRS retention failure depends on the CF growth process driven by ion migration through thermally activated hopping and is described by[22]

$$t_{failure} = \tau \exp\left(\frac{E_a - \alpha q V}{kT}\right), \quad (1)$$

where τ is a constant with unit of time, E_A is the energy barrier for ion hopping, α is the barrier lowering coefficient, q is electronic charge, V is the stress voltage, k is the Boltzmann constant, and T is the device temperature consisting of both the ambient value and the effect of Joule heating. A similar model can be applied for LRS to HRS (reset) retention failure[23].When the device was set to the low resistance state, no failure was observed, in either the F-doped or undoped devices, at any temperature up to 250 °C. Also no failure was observed for any CVS, even close to the reset voltage, during measurement time of 10^5 s. This is attributed to the metallic-like characteristic of the conductive filament which has a relatively low temperature coefficient and a uniform electrical field distribution. Under these circumstances, there is insufficient energy for the oxygen vacancies to migrate away from the filament. This explanation agrees with the literature[23], suggesting that HRS dominates the retention failure. For undoped devices, the retention failure in the high resistance state was only observed at a temperature of 250 °C and when the value of the constant voltage was very close to the set voltage, as shown in Fig. 6. Further increase in stress voltage sets the device immediately. Likewise increasing the temperature above 250 °C showed device degradation (not switching) and even early breakdown. It should also be noted that when the stress voltage (0.4 V) is closer to set voltage (0.45-0.5 V), an abrupt failure occurs, whereas at a stress voltage of 0.35 V the failure is gradual. Verification of the retention failure model and prediction of the retention failure time at room temperature requires measurements at least at three different temperatures. Assuming, however, that the model is valid, by adopting the hopping energy barrier values from the literature, it is possible to estimate the retention failure time at room temperature even with data measured at one temperature. If t_1 and t_2 are the retention failure times at two different temperatures T_1 and T_2, then

$$t_2 = t_1 \exp\left[\frac{E_a - \alpha q V}{kT_2}\left(1 - \frac{T_2}{T_1}\right)\right]. \quad (2)$$

The reported hopping energy barrier values for Ta_2O_5 are in the range 0.3-1 eV[24, 25]. The observed retention time at 250 °C and CVS of 0.4 V is 14,000 s and assuming $\alpha = 0.3$[22], the minimum retention time of 1×10^5 s (1 day) at room temperature and CVS of 0.4 V is estimated. Furthermore, the retention times at two different stress voltages V_1 and V_2 at temperature T can be related as

$$t_2 = t_1 \exp\left[\frac{\alpha q\left(V_1 - V_2\right)}{kT}\right], \tag{3}$$

which gives a further increase by a factor of 100 at zero volts stress (minimum 3.3 months). The F-doped devices do not fail during the measurement time of 10^5 s. Accordingly, a minimum retention failure time of 2 years can be estimated for the F-doped device at room temperature and with no stress.

The enhanced stability of the resistive states and extensive increase in endurance and retention time by F-doping are ascribed to the passivation of oxygen vacancies by F atoms. This reduces the number of oxygen vacancies and reduces the resistive states variability by eliminating the excess conduction paths. The increase in retention failure time is presumably due to an increase in hopping distance between oxygen vacancies and hence increase in hopping energy barrier.

In conclusion, RRAM devices were fabricated by ALD of Ta_2O_5 doped with fluorine. Density functional modeling of the atomic structures and calculation of the density of states using sX hybrid functional correction show that the oxygen vacancies are substituted with F atoms, resulting in the passivation of the oxygen vacancy and removal of the defect state in the midgap of the oxide. The dc and ac sweep set-reset measurements show that passivation of oxygen vacancies increases the switching memory window and state stability, which has been attributed to the elimination of excess conductive filament. The stability of states and the separation of states at various set currents indicated that the device is suitable for MLC switching applications. The devices have set and reset voltages of less than 1 V and their variability is improved by doping. The pulse endurance is increased from 50,000 cycles for undoped to more than one million cycles for F-doped devices.

The work has been funded by the Engineering and Physical Sciences Research Council (EPSRC) UK, project numbers EP/M00662X/1, EP/M009297/1 and EP/M006727/1.

[1]H. Akinaga and H. Shima, Proc. IEEE **98**, 2237 (2010); H. S. P. Wong, H. Y. Lee, S. M. Yu, Y. S. Chen, Y. Wu, P. S. Chen, B. Lee, F. T. Chen, M. J. Tsai, Proc. IEEE **100**, 1951 (2012).

[2]W. Kim, S. Menzel, D. J. Wouters, Y. Guo, J. Robertson, B. Roesgen, R. Waser, and V. Rana, Nanoscale **8**, 17717 (2016); A. Calderoni, S. Sills, C. Cardon, E. Faraoni, N. Ramaswamy, Microelectron. Eng. **147**, 145 (2015); J. J. Yang, M. D. Pickett, X. Li[1], D. A. A. Ohlberg, D. R. Stewart, and R. S. Williams, Nat. Nanotechnol. **3**, 429 (2008); J. J. Yang, M. X. Zhang, J. P. Strachan, F. Miao, M. D. Pickett, R. D. Kelley, G. Medeiros-Ribeiro, and R. S. Williams, Appl. Phys. Lett. **97**, 232102 (2010); U. Celano, L. Goux, R. Degraeve, A. Fantini, O. Richard, H. Bender, M. Jurczak, and W. Vandervorst, Nano Lett. **15**, 7970 (2015).

[3]S. H. Misha, N. Tamanna, J. Woo, S. Lee, J. Song, J. Park, S. Lim, J. Park, and H. Hwang, ECS Solid State Lett. 4, P25 (2015).

[4]W. Kim, S. I. Park, Z. Zhang, and S. Wong, IEEE T. Electron Dev. **61**, 2158 (2014).

[5]H. Xie, Q. Liu, Y. Li, H. Lu, M. Wang, X. Liu, H. Sun, X. Yang, S. Long, S. Liu, and M. Liu , Semicond. Sci. Technol. **27**, 125008 (2012).

[6]N. Sedghi, H. Li, I. F. Brunell, K. Dawson, R. J. Potter, Y. Guo, J. T. Gibbon, V. R. Dhanak, W. D. Zhang, J. F. Zhang, J. Robertson, S. Hall, and P. R. Chalker, Appl. Phys. Lett. **110**, 102902 (2017).

[7]C. H. Cheng, P. C. Chen, Y. H. Wu, M. J. Wu, F. S. Yeh, and A. Chin, Solid State Electron. **73**, 60 (2012).

[8]H. Li, Q. Chen, X. Chen, Q. Mao, J. Xi, and Z Ji, Thin Solid Films **537**, 279 (2013).

[9]T. Tan, T. Guo, and Z. Liu, J. Alloy. Compd. **610**, 388 (2014).

[10]H. Zhang, L. Liu, B. Gao, Y. Qiu, X. Liu, J. Lu, R. Han, J. Kang, and B. Yu, Appl. Phys. Lett. **98**, 042105 (2011).

[11]S. Kim, S. Choi, J. Lee, and W. D. Lu, ACS Nano **8**, 10262 (2014).

[12]J. W. Roberts, P. R. Chalker, K. B. Lee, P. A. Houston, S. J. Cho, I. G. Thayne, I. Guiney, D. Wallis, and C. J. Humphreys, Appl. Phys. Lett. **108**, 072901 (2016).

[13]H. Li, Y. Guo, and J. Robertson, Appl. Phys. Lett. **104**, 192904 (2014).

[14]H. Chen, C. H. Kao, B. Y. Huang, and W. S. Lo, Appl. Surf. Sci. **283**, 694 (2013).

[15]H. H. Tseng, P. J. Tobin, S. Kalpat, J. K. Schaeffer, M. E. Ramón, L. Fonseca, Z. X. Jiang, R. I. Hegde, D. H. Triyoso, and S. Semavedam , IEDM Tech. Dig., 713 (2005); IEEE T. Electron Dev. **54**, 3267 (2007).

[16]C. H. Kao and H. Chen, Jpn. J. Appl. Phys. **51**, 041502 (2012).

[17]Y. Guo and J. Robertson, Appl. Phys. Lett. **104**, 112906 (2014).

[18]Y. Guo and J. Robertson, Microelectron. Eng. **147**, 254 (2015).

[19]S. J. Clark and J. Robertson, Phys. Rev. B **82**, 085208 (2010).

[20]K. Tse and J. Robertson, Appl. Phys. Lett. **89**, 142914 (2006).

[21]T. Schimizu and M. Koyama, Appl. Surf. Sci. **254**, 6109 (2008).

[22]D. Ielmini, IEEE T. Electron Dev. **58**, 4309 (2011).

[23]Y. Koo, S. Ambrogio, J. Woo, J. Song, D. Ielmini, and H. Hwang, IEEE Electr. Device L. **36**, 238 (2015).

[24]B. Gao, H. Zhang, B. Chen, L. Liu, X. Liu, R. Han, J. Kang, Z. Fang, H. Yu, B. Yu, and D. L. Kwong, IEEE T. Electron Dev. **32**, 276 (2011).

[25]Y. Guo and J. Robertson, Appl. Phys. Lett. **105**, 223516 (2014).

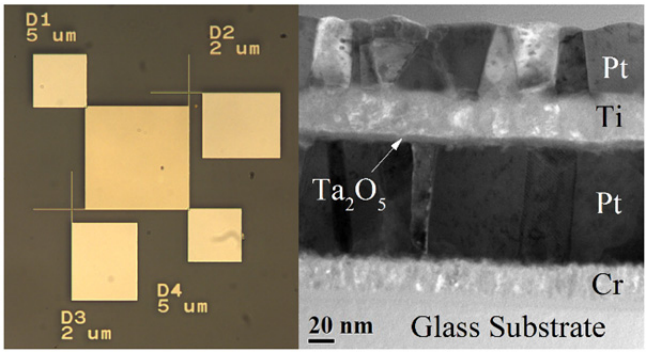

FIG. 1. (Left) Plan view optical microscope image of a group of four devices and (right) the cross section TEM image of a device.

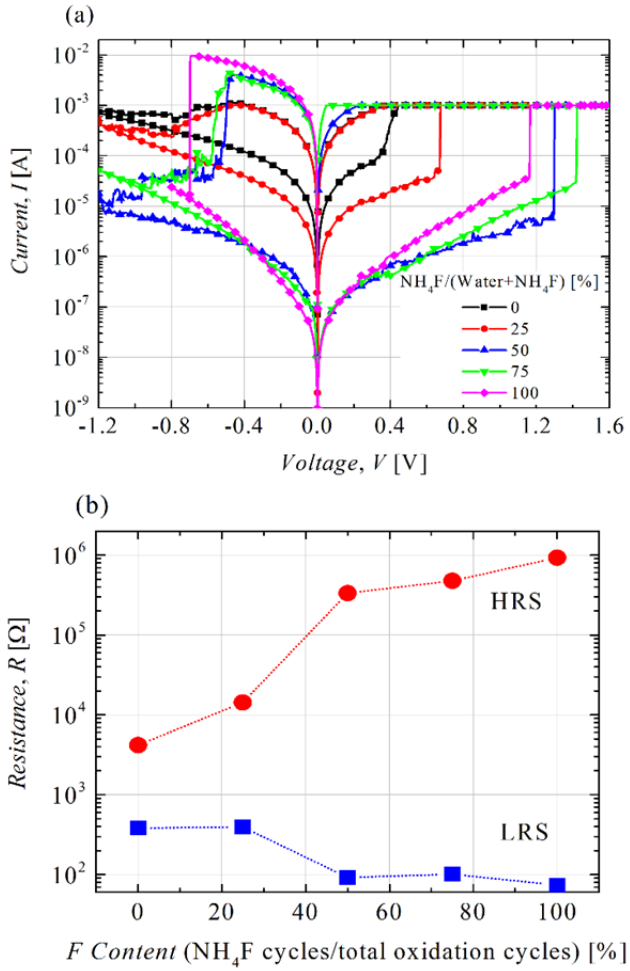

FIG. 2. (a) The dc sweep set and reset cycles on F-doped devices with different percentage of doping, and (b) the variation of HRS and LRS resistance with F doping.

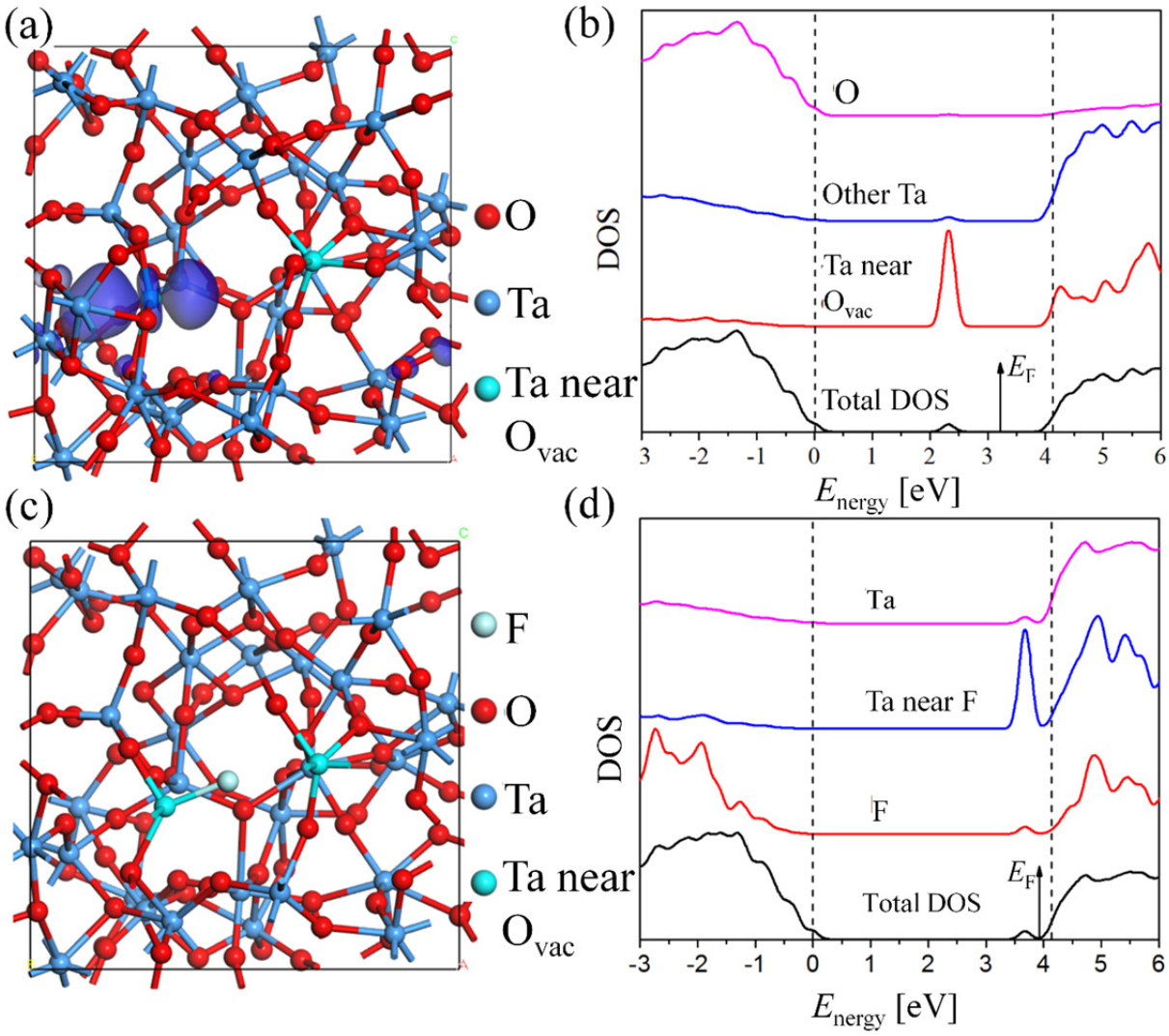

FIG. 3. (a) The O vacancy in amorphous Ta_2O_5 and the defect orbital in mid-gap region; (b) the DOS of amorphous Ta_2O_5 with an O vacancy showing the defect state in the mid-gap; (c) incorporation of a F atom taking the place of O vacancy in the amorphous Ta_2O_5 structure, and (d) the DOS of F-doped Ta_2O_5 showing removal of the O vacancy defect state in mid-gap.

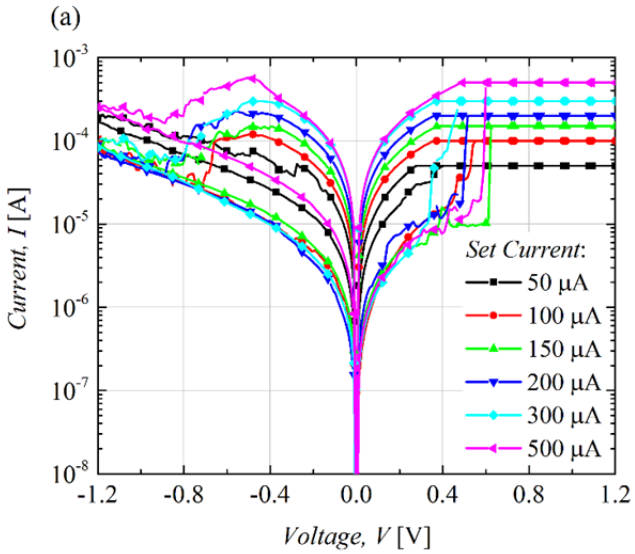
(a)
Current, I [A]
Voltage, V [V]
Set Current:
50 μA
100 μA
150 μA
200 μA
300 μA
500 μA

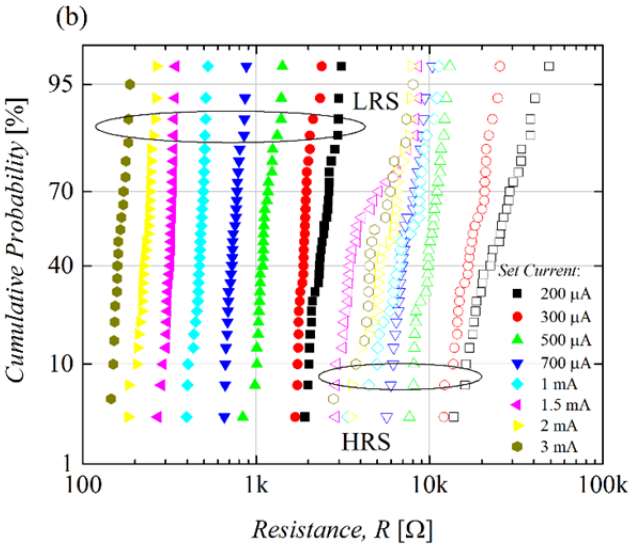
(b)
Cumulative Probability [%]
Resistance, R [Ω]
LRS
HRS
Set Current:
200 μA
300 μA
500 μA
700 μA
1 mA
1.5 mA
2 mA
3 mA

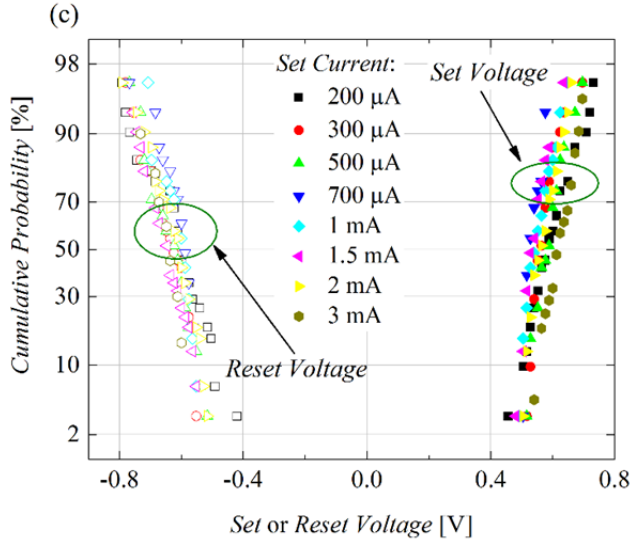
(c)
Cumulative Probability [%]
Set or Reset Voltage [V]
Set Current:
200 μA
300 μA
500 μA
700 μA
1 mA
1.5 mA
2 mA
3 mA
Set Voltage
Reset Voltage

FIG. 4. (a) Variation of switching characteristics on an F-doped device with set current compliance, the cumulative probability distribution of (b) LRS (solid symbols) and HRS (open symbols) resistances at – 0.1 V, and (c) set (solid symbols) and reset (open symbols) voltages.

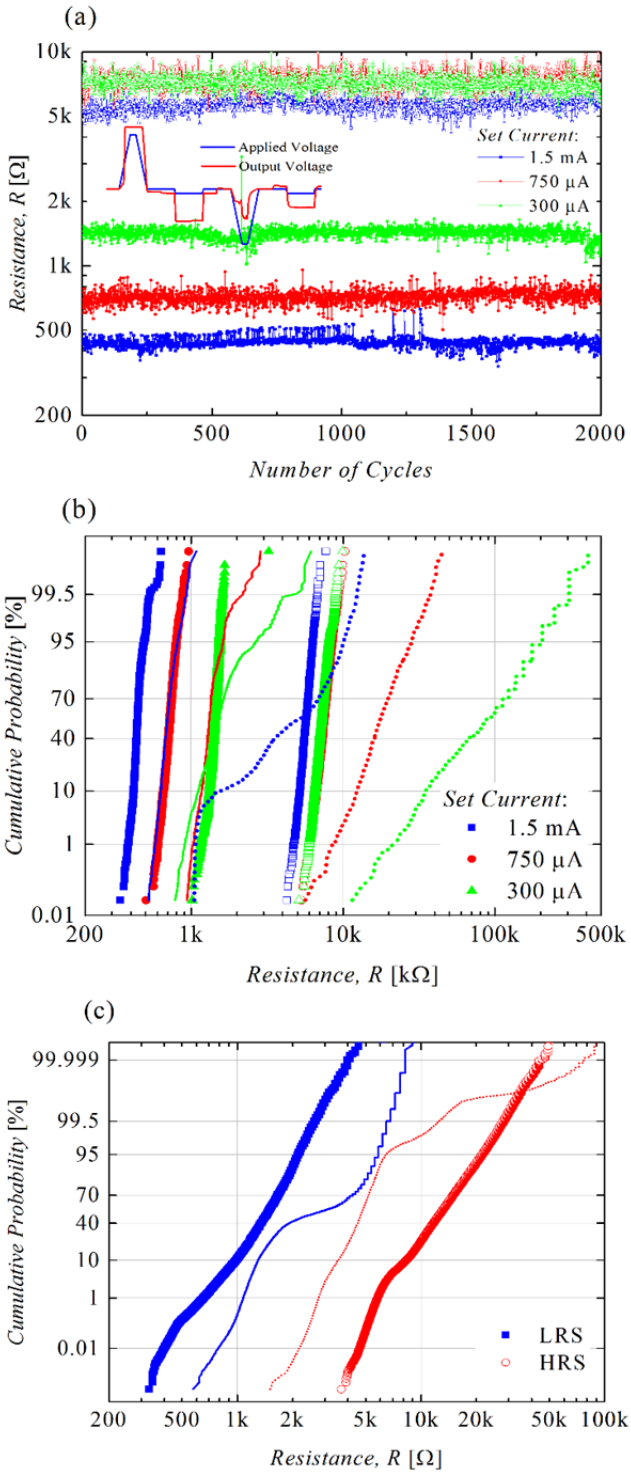

FIG. 5. (a) The HRS and LRS resistances of an F-doped device for 2000 pulsed set and reset cycles (input and output waveforms as inset), (b) the cumulative probability distribution of LRS (solid symbols) and HRS (open symbols) resistances at – 0.1 V, and (c) same as (b) for one million cycles. The corresponding CDF plots for an undoped devices are shown by solid (LRS) and dotted (HRS) lines for comparison.

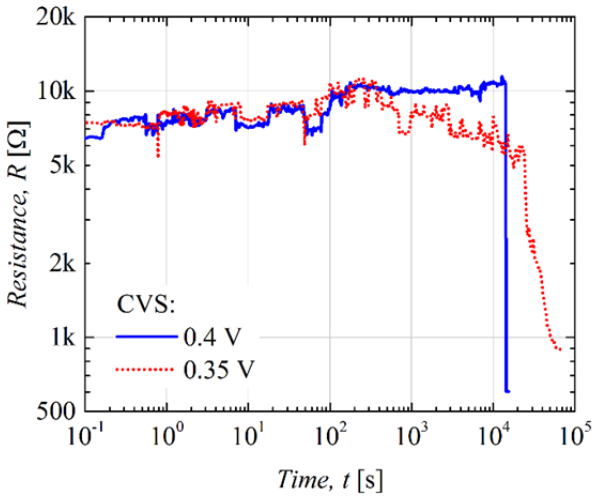

FIG. 6. The HRS retention at 250 °C and at two values of constant voltage stress.

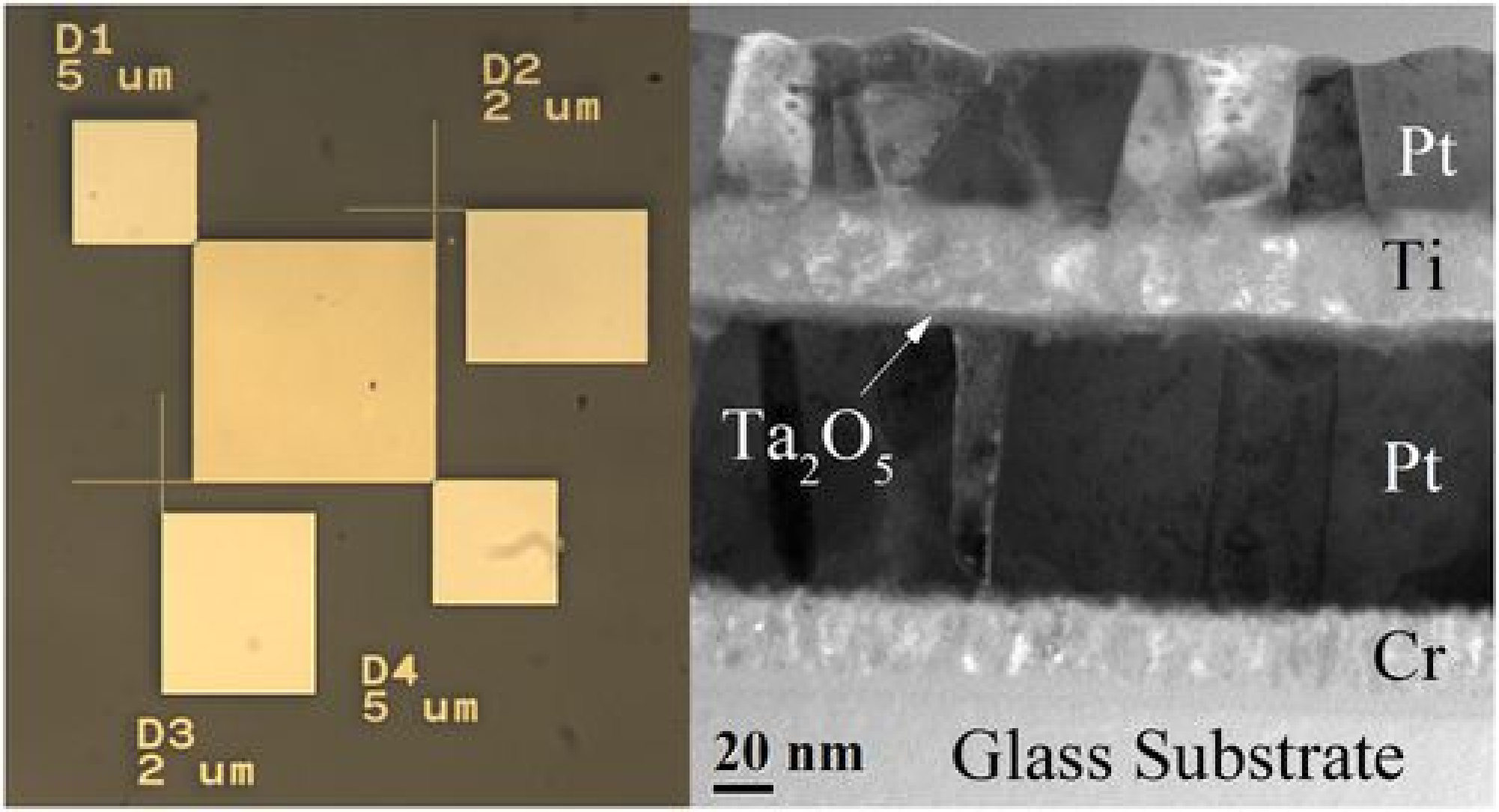
D1
5 um
D2
2 um
D3
2 um
D4
5 um
Pt
Ti
Ta_2O_5
Pt
Cr
20 nm
Glass Substrate

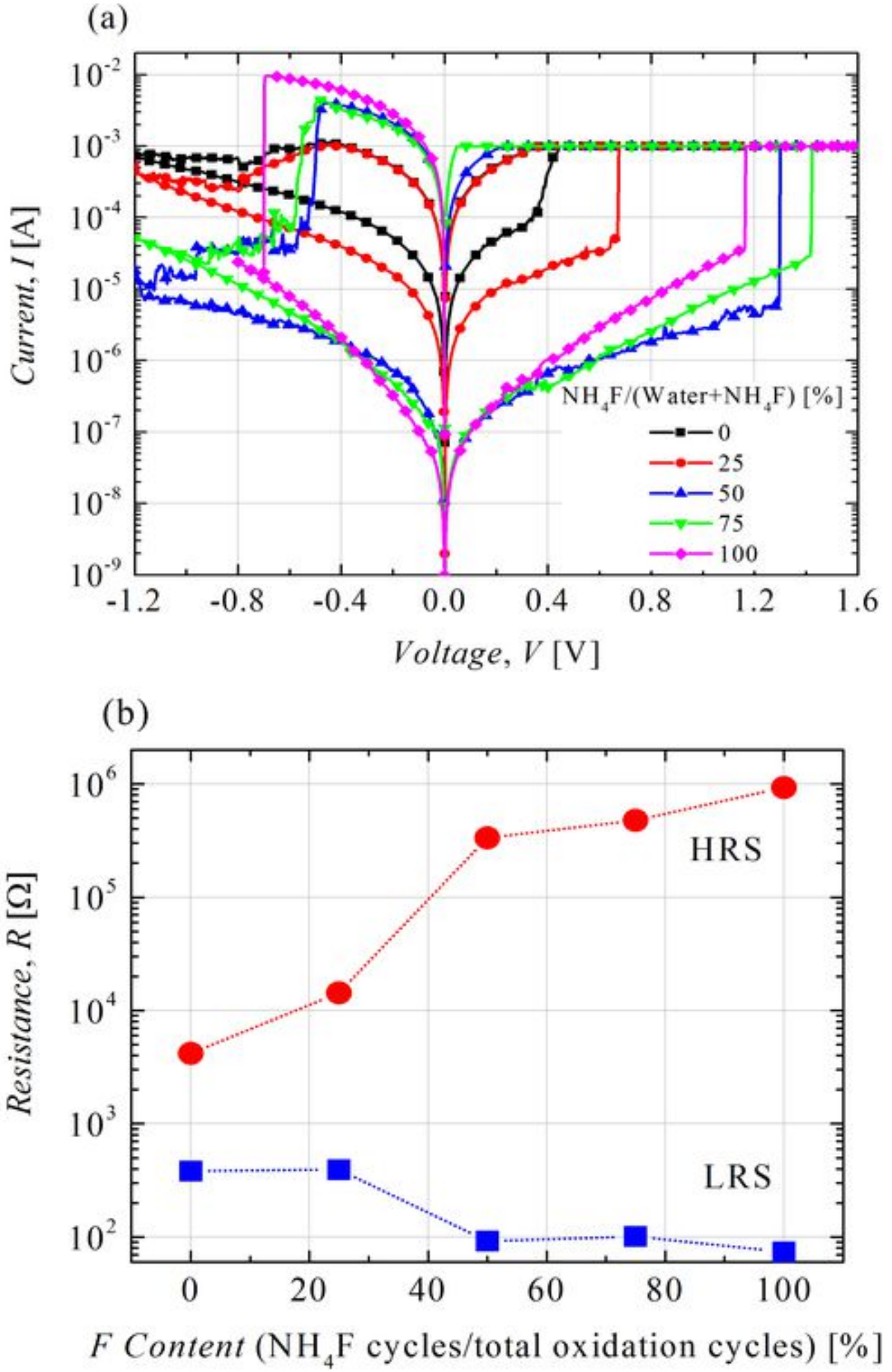
(a)
Current, I [A]
Voltage, V [V]
NH4F/(Water+NH4F) [%]
0
25
50
75
100
(b)
Resistance, R [Ω]
HRS
LRS
F Content (NH4F cycles/total oxidation cycles) [%]

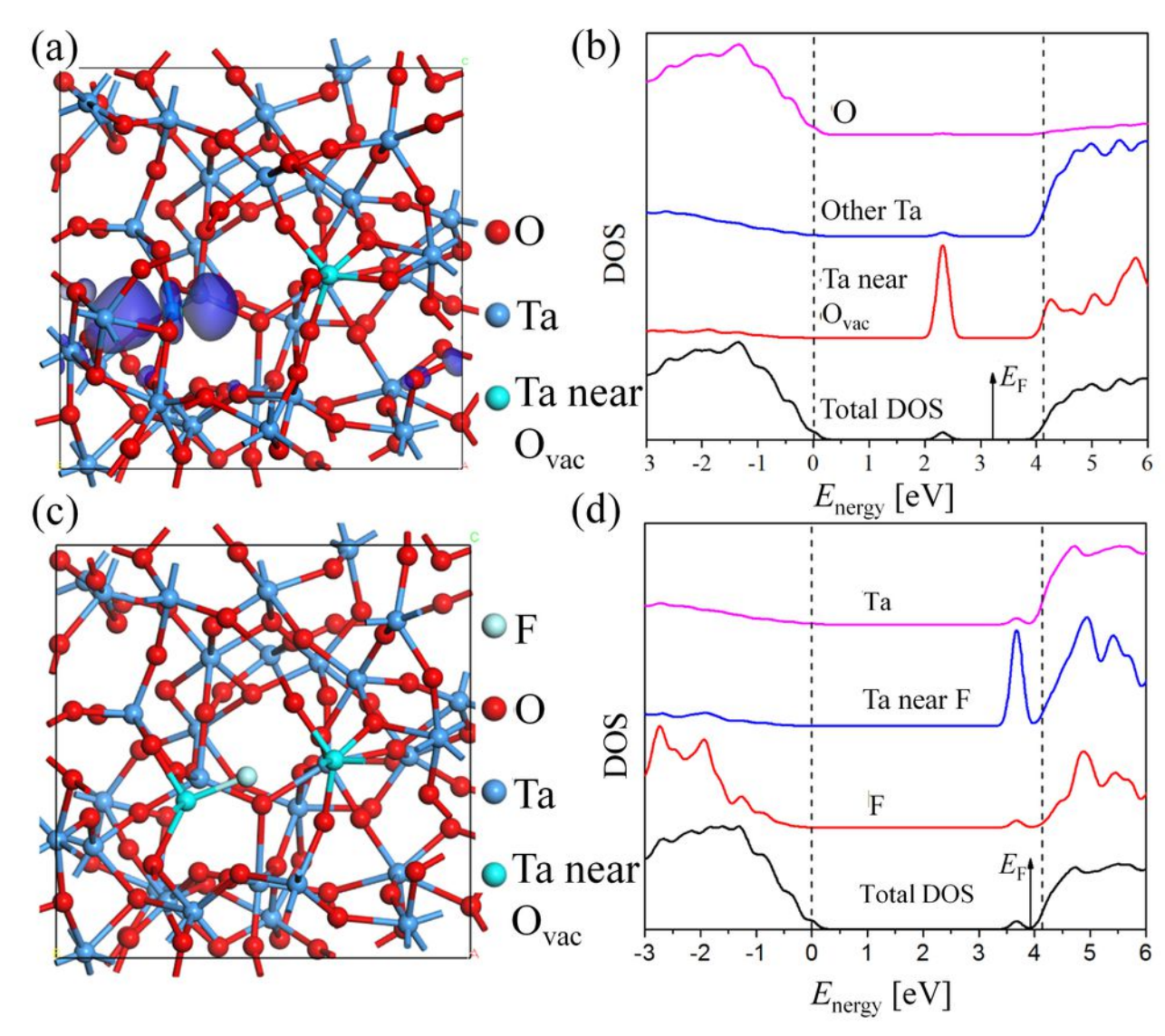
(a)
O
Ta
Ta near
O$_{vac}$
(b)
O
Other Ta
Ta near
O$_{vac}$
Total DOS
E_F
DOS
3 -2 -1 0 1 2 3 4 5 6
E_{nergy} [eV]
(c)
F
O
Ta
Ta near
O$_{vac}$
(d)
Ta
Ta near F
F
Total DOS
E_F
DOS
-3 -2 -1 0 1 2 3 4 5 6
E_{nergy} [eV]

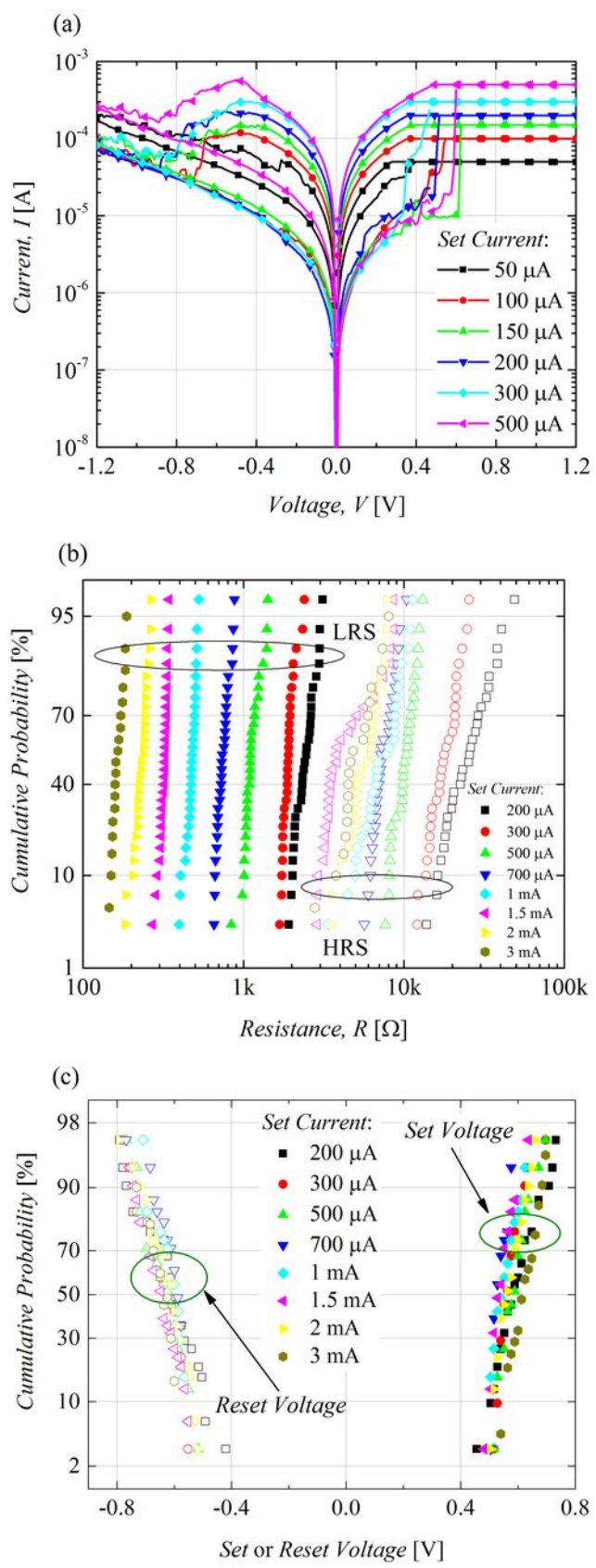
(a)
Current, I [A]
Voltage, V [V]
Set Current:
50 μA
100 μA
150 μA
200 μA
300 μA
500 μA
(b)
Cumulative Probability [%]
Resistance, R [Ω]
LRS
HRS
Set Current:
200 μA
300 μA
500 μA
700 μA
1 mA
1.5 mA
2 mA
3 mA
(c)
Cumulative Probability [%]
Set or Reset Voltage [V]
Set Current:
200 μA
300 μA
500 μA
700 μA
1 mA
1.5 mA
2 mA
3 mA
Set Voltage
Reset Voltage

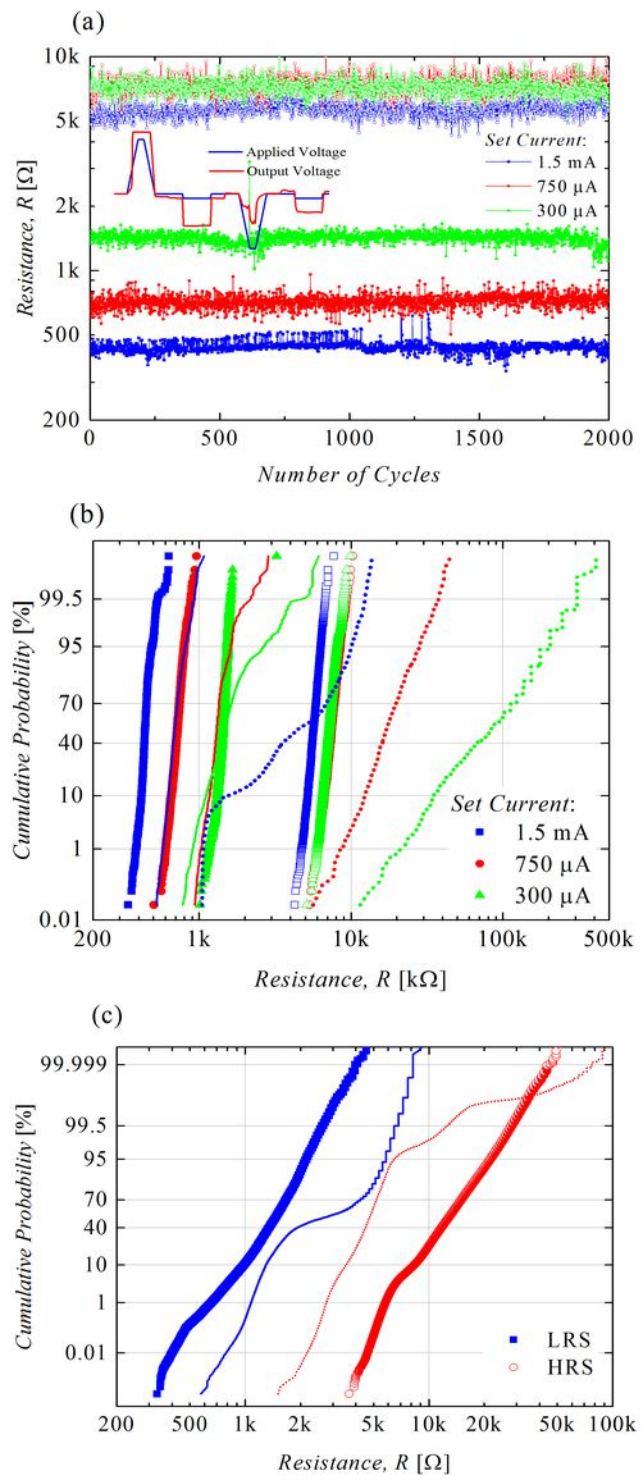
(a)
10k
5k
2k
1k
500
200
Resistance, R [Ω]
Applied Voltage
Output Voltage
Set Current:
1.5 mA
750 μA
300 μA
0
500
1000
1500
2000
Number of Cycles
(b)
99.5
95
70
40
10
1
0.01
Cumulative Probability [%]
Set Current:
1.5 mA
750 μA
300 μA
200
1k
10k
100k
500k
Resistance, R [kΩ]
(c)
99.999
99.5
95
70
40
10
1
0.01
Cumulative Probability [%]
LRS
HRS
200
500
1k
2k
5k
10k
20k
50k
100k
Resistance, R [Ω]

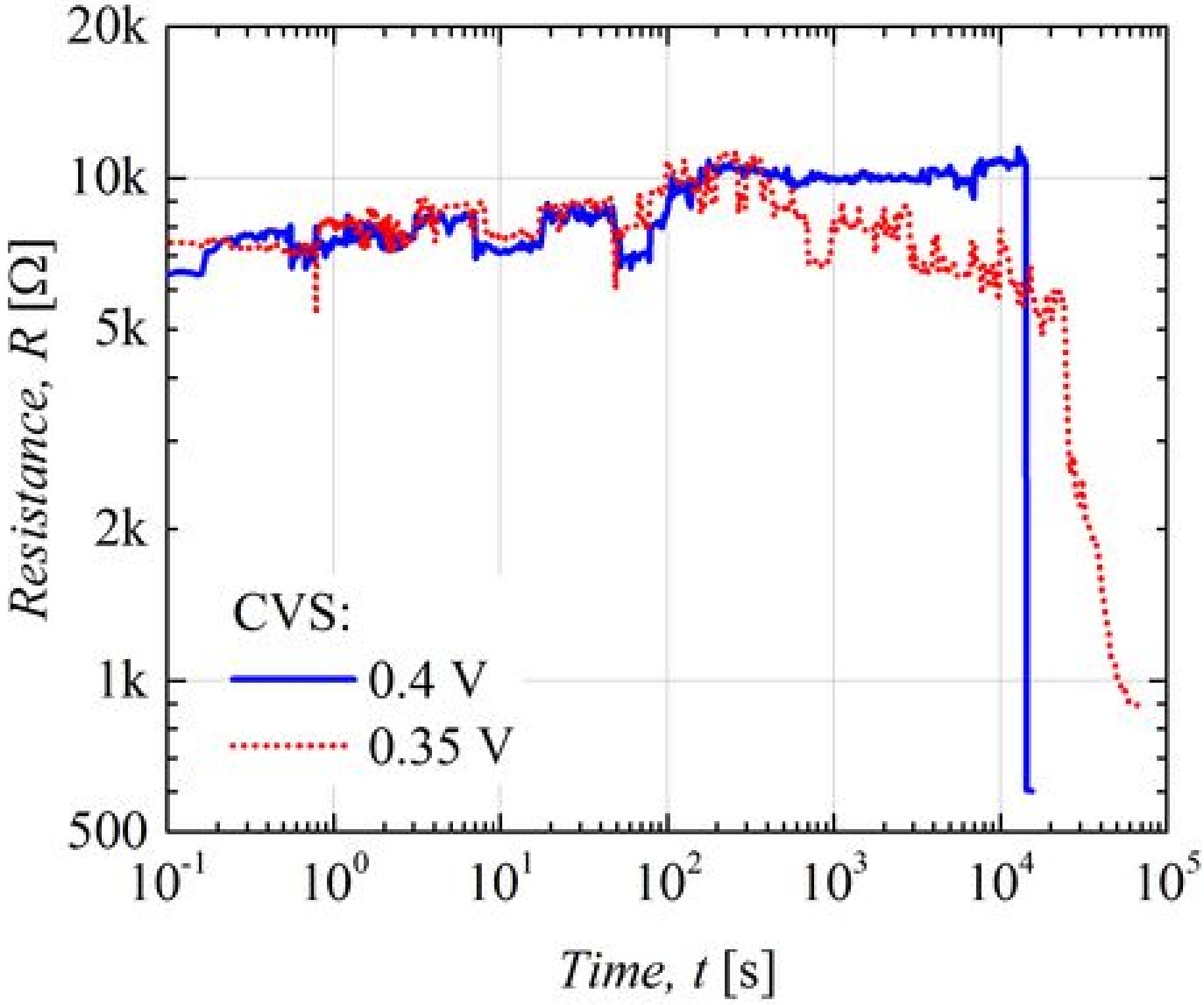
20k
10k
5k
2k
1k
500
Resistance, R [Ω]
CVS:
0.4 V
0.35 V
10^-1
10^0
10^1
10^2
10^3
10^4
10^5
Time, t [s]